Photonic crystals with bound states in continuum and their realization by an advanced digital grading method

2009 J. Phys. A: Math. Theor. 42 415304

(http://iopscience.iop.org/1751-8121/42/41/415304)

IOP PUBLISHING JOURNAL OF PHYSICS A: MATHEMATICAL AND THEORETICAL

J. Phys. A: Math. Theor. **42** (2009) 415304 (15pp) doi:10.1088/1751-8113/42/41/415304

Photonic crystals with bound states in continuum and their realization by an advanced digital grading method

N Prodanović, V Milanović and J Radovanović

Faculty of Electrical Engineering, University of Belgrade, Bulevar Kralja Aleksandra 73, 11120 Belgrade, Serbia

E-mail: radovanovic@etf.bg.ac.yu

Received 20 April 2009, in final form 26 August 2009
Published 29 September 2009
Online at stacks.iop.org/JPhysA/42/415304

Abstract

The Helmholtz equation can be reshaped into a form analogous to the Schrödinger equation with the term labeled 'the optical potential'. By following this analogy, we conclude that there exist certain profiles of optical potentials which possess bound states of electric field in the continuous part of the spectrum. One of the methods for generating these specific optical potentials is the application of supersymmetric formalism which transforms a real (initial) potential into a family of complex potentials, which all have one bound state in the continuum. We present general steps of this procedure and illustrate its use through the example of flat initial optical potential. In this particular case, conditions are found for the existence of the bound field in continuum, as well as the expression for the field and the corresponding complex optical potential in an analytic form. In addition, the approximation of digital grading is applied to the generated complex supersymmetric optical potential and the 'bound' state is calculated. The complex nature and the sharp variations of the supersymmetric optical potential impose the development of an original and sophisticated method of digital grading.

PACS numbers: 11.30.Pb, 03.65.Ge, 42.25.Bs

1. Introduction

Von Neumann and Wigner [1] were the first to find that the Schrödinger equation may have regular solutions which represent bound states in the continuous part of the spectrum. They have modulated the wavefunction in order to make it normalizable, and then used the modulating function to extract the potential which supports such states. Herrick and Stillinger [2–4] have shown that bound states in continuum may exist in atoms and molecules, and also

pointed to the possibility of an electron in the electric field becoming localized by addition of a suitable potential. Starting from a separable form of the Hamiltonian, Robnik has also derived normalizable wavefunctions [5]. While the existence of normalizable eigensolutions for non-local potentials is rather well explored [6], a systematic approach for local potentials is still missing. Various techniques have been employed for the wavefunction modulation [7]. In [8], the authors give an experimental demonstration of resonant states in continuum which are fairly similar in nature to bound states in continuum.

The physical phenomenon of bound states in continuum appears only for particular potential profiles, either in the quantum mechanical or optical case. In addition to above techniques for generating these specific potentials which support discrete states in continuous part of the spectrum, supersymmetric quantum mechanics (SUSYQM) represents a very efficient method which has primarily been used in quantum mechanical problems, and less often in optical problems. However, applying SUSYQM to a potential that is real leads to bound states only on the half-line $x \in (0, \infty)$ [9–11], but not the full line. In order to remove this constraint and generate bound states on the full line, complex potentials are introduced [12, 13]. This, on the other hand, leads to a specific problem with the practical realization of these generated complex potentials.

There is, indeed, a close analogy between quantum mechanical and electromagnetic phenomena. In [14], the existence of bound states in radiation continuum is illustrated in the example of two parallel gratings and two arrays of thin parallel cylinders, while [15, 16] show that photonic crystals with defects may have localized states in the continuous part of the spectrum.

In this paper, we start from the modified form of the Helmholtz equation for the electric field, which is analogous to the Schrödinger equation (and so are their general solutions), in order to construct complex optical potentials isospectral with the selected initial one. Each of the complex optical potentials supports one and only one localized normalizable function of the electric field in the continuum part of the spectrum. We first give a brief description of the SUSY procedure, details of which can be found in [12, 13], applied to a quantum mechanical problem, and then implement it to the case of a flat optical potential. Finally, we present the somewhat non-standard digital grading approximation of the generated complex potential and numerical solution for the electrical field function corresponding to it, with satisfactory similarity to the original solution.

2. Theoretical considerations

Consider a material that is linear and non-homogeneous in the x-direction, described by the following equations:

$$\begin{aligned} \overrightarrow{D} &= \varepsilon(x)\varepsilon_0 \overrightarrow{E} \\ \overrightarrow{B} &= \mu(x)\mu_0 \overrightarrow{H}. \end{aligned} \tag{1}$$

In addition, two practical restrictions are imposed: (1) the EM waves are propagating along the z-direction and (2) only the TE modes are considered, i.e. $\overrightarrow{E} = E\overrightarrow{e_y}$.

The propagation of monochromatic waves with frequency ω_0 is governed by the scalar wave equation which for the case of the TE modes may be written for the y component of the electric field:

$$-\frac{\partial^2 E(x,z)}{\partial z^2} - \frac{\partial^2 E(x,z)}{\partial x^2} + \frac{1}{\mu}\frac{\mathrm{d}\mu}{\mathrm{d}x}\frac{\partial E(x,z)}{\partial x} - \frac{\varepsilon(x)\mu(x)}{c^2}\omega_0^2 E(x,z) = 0. \tag{2}$$

This equation is solved by separation of variables, i.e. by taking $E(x, z) = E(x)E(z)$ and subsequently inserting

$$E(x) = \sqrt{\mu(x)}u(x), \tag{3}$$

into the Helmholtz equation, which thus becomes

$$-\frac{\mathrm{d}^2u(x)}{\mathrm{d}x^2} + \left[-k_0^2\varepsilon(x)\mu(x) - \frac{1}{2\mu}\frac{\mathrm{d}^2\mu(x)}{\mathrm{d}x^2} + \frac{3}{4}\frac{1}{\mu^2(x)}\left(\frac{\mathrm{d}\mu(x)}{\mathrm{d}x}\right)^2\right]u(x) = -\beta^2u(x). \tag{4}$$

where $k_0 = \omega_0/c$ and β is the propagation constant. Furthermore, it is convenient to introduce a new function called 'the optical potential', which is defined as

$$\Theta(x) = -k_0^2\varepsilon(x)\mu(x) - \frac{1}{2\mu}\frac{\mathrm{d}^2\mu(x)}{\mathrm{d}x^2} + \frac{3}{4}\frac{1}{\mu^2(x)}\left(\frac{\mathrm{d}\mu(x)}{\mathrm{d}x}\right)^2. \tag{5}$$

In this manner equation (4) becomes analogous to the Schrödinger equation $-\frac{\hbar^2}{2m}\frac{\mathrm{d}^2\psi(x)}{\mathrm{d}x^2} + U(x)\psi(x) = E\psi(x)$, and takes the form

$$-\frac{\mathrm{d}^2u(x)}{\mathrm{d}x^2} + \Theta(x)u(x) = \nu u(x) \tag{6}$$

where $\nu = -\beta^2$. It can easily be shown that the functions $\frac{1}{\mu(x)}\frac{\mathrm{d}E(x)}{\mathrm{d}x}$ and $E(x)$ are continuous if $\varepsilon(x)$ and $\mu(x)$ have only finite discontinuities. Hence, the quantities $\sqrt{\mu(x)}u(x)$ and $\frac{1}{\sqrt{\mu(x)}}\frac{\mathrm{d}u(x)}{\mathrm{d}x} + \frac{u(x)}{2\mu^{3/2}(x)}\frac{\mathrm{d}\mu}{\mathrm{d}x}$ must also be continuous. The last equation may be rewritten in the operator form as

$$\widehat{\mathrm{N}}u = \nu u \tag{7a}$$

$$\widehat{\mathrm{N}} = -\frac{\mathrm{d}^2}{\mathrm{d}x^2} + \widehat{\Theta}. \tag{7b}$$

The operator $\hat{N}$ is a Hermitian operator and can be written as

$$\widehat{\mathrm{N}} = \widehat{A_2}\widehat{A_1} + \nu \tag{8}$$

where ν is an arbitrary eigenvalue of the operator $\widehat{\mathrm{N}}$, and the operators $\widehat{A_1}$ and $\widehat{A_2}$ are defined as

$$\widehat{A_1} = \frac{\mathrm{d}}{\mathrm{d}x} + \widehat{W} \tag{9a}$$

$$\widehat{A_2} = -\frac{\mathrm{d}}{\mathrm{d}x} + \widehat{W}. \tag{9b}$$

Here the term $\widehat{W}$ denotes the 'optical superpotential':

$$\widehat{W}(x) = -\frac{1}{\overline{u_v}(x)}\frac{\mathrm{d}\overline{u_v}(x)}{\mathrm{d}x}. \tag{10}$$

In this equation,

$$\overline{u_v}(x) = u_v(x)\left[1 + C\int_{(x)}\frac{\mathrm{d}x}{u_v^2(x)}\right] \tag{11}$$

is a general solution of the starting eigenproblem for the eigenvalue ν. The presence of the constant C is an indication of degeneracy of any solution of (4). In standard methods of solving of equation (4) it is usually assumed that the fields are finite and square integrable so in some cases the values of C become fixed. In the SUSY procedure applied here, the

nature of (11) is not significant because it is just an intermediate result which will be used for construction of some other solution of another optical potential with desired properties. Thus, it is not necessary to impose any restrictions on the complex constant C at this stage. The central property that is required of the end solution is its square integrability and localization in space, in spite of the fact that the corresponding eigenvalue belongs to the continuous part of the spectrum. Hence, the appropriate limitations to the values of C will be enforced once the final electric field function is obtained.

By following the conventional SUSY procedure we next consider the operator

$$\widehat{\mathrm{N}}_2 = \widehat{A_1}\widehat{A_2} + \nu = -\frac{\mathrm{d}^2}{\mathrm{d}x^2} + \widehat{\Theta}_2. \tag{12}$$

As the constant C is a complex number here, so is the potential $\widehat{\Theta}_2$, and the new operator is thus non-Hermitian. Yet, it is isospectral to the initial Hamiltonian, with the exception of ν which is not its eigenvalue. We continue in an analogous manner, by constructing the operator $\widehat{\mathrm{N}}_3$:

$$\widehat{\mathrm{N}}_3 = \widehat{\overline{A_2}}\widehat{\overline{A_1}} + \nu = -\frac{\mathrm{d}^2}{\mathrm{d}x^2} + \widehat{\Theta}_3, \tag{13}$$

which is defined via the new optical superpotential:

$$\overline{W}(x) = -\frac{1}{\overline{u_{v2}}(x)}\frac{\mathrm{d}\overline{u_{v2}}(x)}{\mathrm{d}x}. \tag{14}$$

Here $\overline{u_{v2}}(x)$ represents a general eigenvector of the operator $\widehat{\mathrm{N}}_2$:

$$\overline{u_{v2}}(x) = \frac{1}{\overline{u_v}(x)}\left[\rho + \int_{(x)} \overline{u}_v^2(x)\mathrm{d}x\right] \tag{15}$$

corresponding to the eigenvalue v, where ρ is an arbitrary constant. The operators $\widehat{\overline{A_1}}$ and $\widehat{\overline{A_2}}$ have the same form as $\widehat{A_1}$ and $\widehat{A_2}$, but with the new superpotential $\overline{W}(x)$ instead of $W(x)$. The optical potential $\widehat{\Theta}_3$ is given by

$$\widehat{\Theta}_{\mathrm{SS}}(x) = \widehat{\Theta}_3(x) = \widehat{\Theta}(x) - 2\frac{\mathrm{d}^2}{\mathrm{d}x^2}\left[\ln(\rho + I(x))\right] \tag{16}$$

where

$$I(x) = \int_{(x)} \overline{u}_v^2(x)\,\mathrm{d}x. \tag{17}$$

The eigenfunction of the operator $\widehat{\mathrm{N}}_3$ for the eigenvalue ν is given by

$$u_{v3}(x) = C_{v3}\frac{\overline{u_v}(x)}{\rho + I(x)} \tag{18}$$

and for any other eigenvalue ν_n the corresponding expression reads

$$u_{3n} = C_{3n}\left((\nu_n - \nu)u_n(x) + \frac{\overline{u_v}(x)\left[\overline{u_v}(x)\frac{\mathrm{d}u_n(x)}{\mathrm{d}x} - u_n\frac{\mathrm{d}\overline{u_v}(x)}{\mathrm{d}x}\right]}{\rho + I(x)}\right). \tag{19}$$

Equation (18) can actually be included in this last formula by considering the limit $\nu_n \to \nu$. The term $(\nu_n - \nu)u_n(x)$would thus vanish, while the limit of the second term in parentheses can be calculated as (see the appendix for details)

$$\frac{\overline{u_v}(x)\left[\overline{u_v}(x)\frac{\mathrm{d}u_n(x)}{\mathrm{d}x} - u_n\frac{\mathrm{d}\overline{u_v}(x)}{\mathrm{d}x}\right]}{\rho + I(x)} \longrightarrow \frac{\overline{u_v}(x)}{\rho + I(x)}. \tag{20}$$

All the eigenfunctions within the discrete part of the spectrum of $\widehat{N}$ are localized in space, in contrast to any of those belonging to the continuum part of the spectrum. The situation is somewhat different for the operator $\widehat{N}_3$ because it may have a localized normalizable eigenvector even for an eigenvalue from the continuum of $\widehat{N}$. This will be illustrated through specific examples. Clearly, the values which are not the eigenvalues of $\widehat{N}$ are not the eigenvalues of $\widehat{N}_3$, either [4].

In this work we consider the following conditions which may have practical relevance: the initial optical potentials are taken to be purely real and variable within a given interval $(x_{\min}, x_{\max})$ but flat (having a constant value C_1) outside of this interval. As a result, within the SUSY treatment we have

$$\overline{u_v}(x \to \pm\infty) \to C_2 \cos(kx) + \sin(kx), \tag{21a}$$

$$I(x \to \pm\infty) \to \frac{x}{2}\left[C_2^2 + 1\right], \tag{21b}$$

$$u_{v3}(x \to \pm\infty) = \frac{C_2 \cos(kx) + \sin(kx)}{\rho + \frac{x}{2}\left[C_2^2 + 1\right]}, \tag{21c}$$

$$\Theta_3(x \to \pm\infty) = C_1. \tag{21d}$$

The last expression indicates that the outer ('flat') segments of the final structure $\Theta_3(x)$ consist of the same material selected for the construction of the initial profile $\Theta(x)$. If the parameters C and ρ are chosen so that the function $\rho + I(x)$ has no zeros on the whole domain, then $u_{v3}(x)$ can be normalized. This will result in certain restrictions imposed on the values of C and ρ. On the other hand, all the other eigenfunctions from the continuous part of the spectrum are not localized (except in the limit $\nu_n \to \nu$), so the final supersymmetric optical potential supports only one bound state in continuum.

In the case of supersymmetric transformation via the (initially) bound state (which is not of interest here), if the parameters C and ρ are both real, the final field can be normalized only for $C = 0$. This is the standard SUSY procedure which results in a real optical potential $\Theta_3(x)$. By observing equation (21*c*) we deduce that, if the constant $C = C_r + \mathrm{i}C_i$ is real ($C_i = 0$ and C_r nonzero), then for any value of ρ one can find a coordinate x at which the denominator $\rho + I(x)$ becomes equal to zero; hence the field function becomes non-normalizable. If C is truly complex and ρ is real, the requirement for the normalizability of the field will determine the acceptable values of these parameters, as will be exemplified below. We will limit our considerations to $\rho \in R$, without any loss of generality, as the case of complex ρ can be analyzed in an analogous manner.

It can also be noted (within our model where the initial potential is real) that the reflection and transmission coefficients remain the same after employing the SUSY formalism. This is due to the fact that all the states wavefunction corresponding to eigenvalues $\nu_n \neq \nu$ have the asymptotic form for $x \to \pm\infty$ which is the same as the form of the wavefunction of the initial potential (for $x \to \pm\infty$). The state corresponding to the eigenvalue ν, as already demonstrated, has one discrete solution (bound state in continuum) and one non-integrable solution which diverges as $x \to \pm\infty$. Therefore, it makes no sense to discuss the transmission and reflection for the state with the eigenvalue ν of the final potential. Finally, if the initial potential is real, the absorption is clearly equal to zero; consequently, the absorption in all the complex final potentials remains zero, which can be expressed by the following equation:

$$\int_{-\infty}^{\infty} \mathrm{Im}(\Theta_{ss}(x))|u_v(x)|^2 \,\mathrm{d}x = 0. \tag{22}$$

At the end of this section, some comments need to be made about the normalization of the function $E_y(x)$. Contrary to the analogous quantum-mechanical problem, in the optical

domain there is no unique solution. One approach to normalization of $E_y(x)$ is by using the time-averaged incident power $P_{\text{in}} = \frac{\gamma_0 \varepsilon_0 c^2 S}{2\omega}|E_0|^2$, where $E_{\text{in}} = E_0\,\mathrm{e}^{\mathrm{i}\gamma_0 x}$, S is the cross-section surface and c is the speed of light in vacuum. If P_{in} is known in advance, assuming that it remains unchanged in the supersymmetric procedure, it is possible to determine E_0 and thus perform the normalization. This is achievable only for continuous states. In the case of discrete states (such as the bound state in continuum), the normalization may be carried out using the method described in [17, 18]. Although it is evident from the above discussion that the normalization of $E_y(x)$ is not unambiguous, it has no considerable importance to the problems considered in this paper.

2.1. Construction of the supersymmetric optical potential via a flat initial optical potential

We examine the case of an optically homogeneous medium characterized by the electric and magnetic permeability ε, and μ, respectively. The selection of the initial potential is made based on its simplicity—the flat potential is clearly the simplest possible choice. Thus, all the terms containing derivatives of $\mu(x)$ in equation (4) vanish, and the product $\varepsilon(x)\mu(x)$ is constant. Certainly, there are many other options for the initial potential, but these would lead to quite complex (if at all obtainable in an analytic form) expressions for $u(x)$, without adding noticeably to the quality of the example. The general solution of (4) is then given by

$$\overline{u}_k(x) = \sin(kx) + C\cos(kx) \tag{23}$$

where

$$k = \sqrt{k_0^2\varepsilon\mu - \beta^2}. \tag{24}$$

Clearly, the spectrum of the flat potential is completely continuous for $\beta^2 < k_0^2\varepsilon\mu$. The aim is to employ the SUSY approach to find the complex potential that accommodates a bound state at the given eigenvalue. The final function can be express as

$$u_{ss}(x) \cong \frac{C\cos(kx) + \sin(kx)}{\rho + \frac{x}{2} - \frac{\sin(2kx)}{4k} - \frac{C\cos^2(kx)}{k} + C^2\left[\frac{x}{2} + \frac{\sin(2kx)}{4k}\right]} \tag{25a}$$

while the superymmetric electric field reads

$$E_{\text{ss}}(x) = \sqrt{\mu}u_{\text{ss}}(x). \tag{25b}$$

The corresponding supersymmetric optical potential is given by

$$\Theta_{\text{ss}}(x) = -k_0^2\varepsilon\mu - 2\frac{\mathrm{d}^2}{\mathrm{d}x^2}\left[\ln\left[\rho + \frac{x}{2} - \frac{\sin(2kx)}{4k} - \frac{C\cos^2(kx)}{k} + C^2\left(\frac{x}{2} + \frac{\sin(2kx)}{4k}\right)\right]\right]. \tag{26}$$

It is evident that the fulfillment of the normalizability conditions for the electric field depends on the denominator of equation (25), which may be separated into real and imaginary parts as

$$\mathrm{Re}(\rho + I(x)) = \rho + \frac{x}{2} - \frac{\sin(2kx)}{4k} - \frac{C_r\cos^2(kx)}{k} + \left(C_r^2 - C_i^2\right)\left[\frac{x}{2} + \frac{\sin(2kx)}{4k}\right] \tag{27a}$$

$$\mathrm{Im}(\rho + I(x)) = -\frac{C_i\cos^2(kx)}{k} + 2C_iC_r\left[\frac{x}{2} + \frac{\sin(2kx)}{4k}\right]. \tag{27b}$$

If $C_i = 0$, then $\mathrm{Im}(\rho + I(x)) = 0$ for every x, and $\mathrm{Re}(\rho + I(x))$ has at least one singularity for any ρ. Further, if $C_i \neq 0$, the equation $0 = -\frac{\cos^2(kx_0)}{k} + 2C_r\left[\frac{x}{2} + \frac{\sin(2kx_0)}{4k}\right]$ can be solved

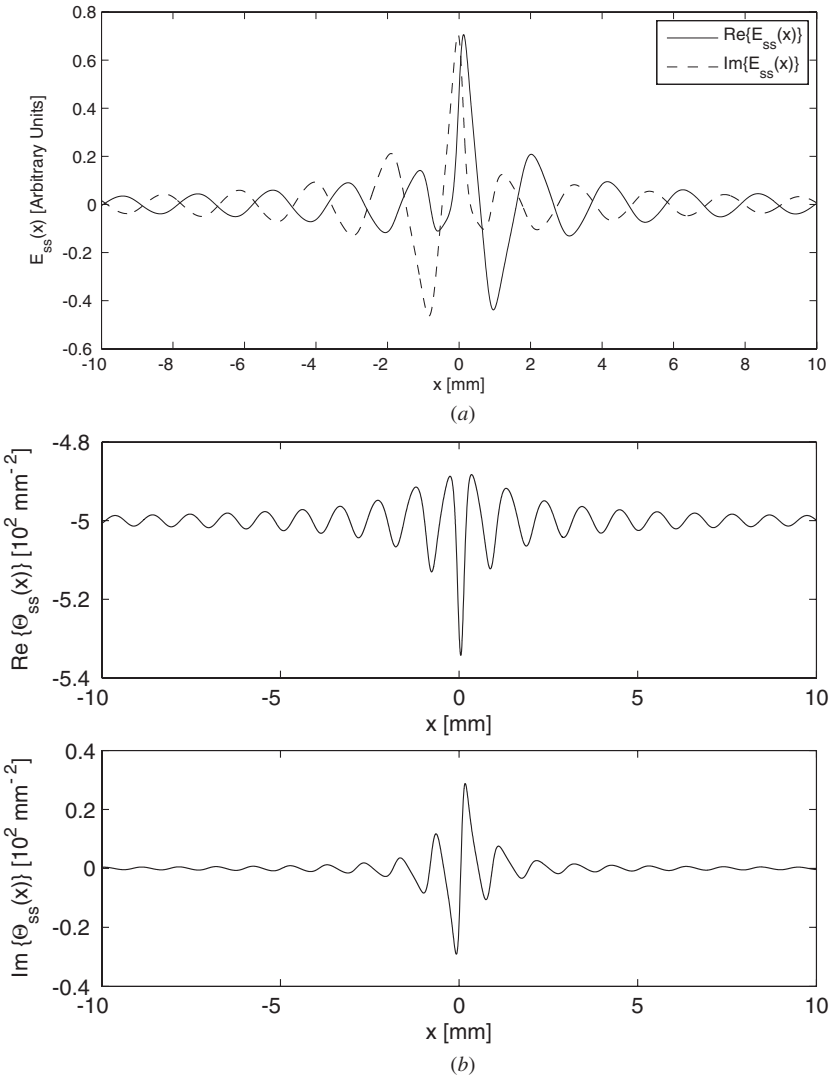

Figure 1. (*a*) An example of the supersymmetric localized electric field; (*b*) the corresponding supersymmetric optical potential, for $C = 3 + 3\mathrm{i}$, $\rho = 6$ mm, $k = 3\ \mathrm{mm}^{-1}$, $k_0^2\varepsilon\mu = 500\,\mathrm{mm}^{-2}$.

for x_0 which cancels out the imaginary part of the system (27), leading to the condition $-\rho \neq \frac{x_0}{2} - \frac{\sin(2kx_0)}{4k} - \frac{C_r\cos^2(kx_0)}{k} + \left(C_r^2 - C_i^2\right)\left[\frac{x_0}{2} + \frac{\sin(2kx_0)}{4k}\right]$ for the real part.

The function $E_{\mathrm{ss}}(x)$ will be square integrable if the coefficient in front of x in the system (27) is non-zero, which will be true if [12, 13]

$$\left(C_iC_r \neq 0 \quad \text{and/or} \quad C_r^2 - C_i^2 + 1 \neq 0\right).$$

After defining the acceptable values for C and ρ, it is straightforward to obtain the family of supersymmetric optical potentials $\Theta_{\mathrm{ss}}(x, \rho, C)$ with corresponding bound supersymmetric electric fields $E_{\mathrm{ss}}(x, \rho, C)$ at the eigenvalue ν. One particular case is shown in figure 1.

As expected from equation (21), the limit of the average value of the complex function $\Theta_{\mathrm{ss}}(x \to \infty)$ amounts to $k_0^2\varepsilon\mu = 500\ \mathrm{mm}^{-2}$.

Numerical results indicate that for lower values of the parameter C and higher values of the parameter ρ, the optical potential and the electric field have lower surges, while these become stronger with the increase of C and the decrease of ρ.

The ultimate goal is to enable practical realization, i.e. to construct a photonic crystal with permittivity $\varepsilon_{\mathrm{SS}}(x)$ and permeability $\mu_{\mathrm{SS}}(x)$ which supports such a bound state in continuum. Obviously, the most direct approach is to devise a material with $\varepsilon_{\mathrm{SS}}(x)$ and $\varepsilon_{\mathrm{SS}}(x)$ so that the resultant optical potential emulates the supersymmetric optical potential obtained previously. There are an infinite number of solutions to this problem. For example, one can apply the digital grading approximation directly to the supersymmetric optical potential and then compose very accurately the obtained digitally graded function.

Nevertheless, if we assume $\mu_{\mathrm{ss}}(x) = \mathrm{const} = \mu_{\mathrm{ss}}$, then according to relation (5) we find

$$\varepsilon_{\mathrm{ss}}(x) = -\frac{\lambda_0^2}{4\pi^2\mu_{\mathrm{ss}}}\Theta_{\mathrm{ss}}(x). \tag{28}$$

We have decided on a nonmagnetic material ($\mu_{\mathrm{SS}} = 1$) for the following reason: in practical realizations, it is much easier to find a set of materials with prescribed real and imaginary parts of the dielectric permittivity, than a set of materials with both the required permittivity and magnetic permeability at given frequency. Regarding the theoretical design of a photonic crystal with the bound state in continuum, it is not significantly more complicated to consider materials with different magnetic permeabilities, as well.

The last expression describes the complex relative permittivity $\varepsilon_{\mathrm{ss}}(x)$, which will be referred to as supersymmetric relative permittivity, proportional to the supersymmetric optical potential. Apparently, photonic crystal with the relative permittivity $\varepsilon(x) = \varepsilon_{\mathrm{ss}}(x)$ and the relative permeability $\mu_{\mathrm{ss}} = 1$ would provide $\Theta(x) = \Theta_{\mathrm{ss}}$, together with the projected bound state in continuum. Thus, the problem is reduced to constructing the suitable photonic crystal with $\varepsilon(x) = \varepsilon_{\mathrm{ss}}(x)$. The approximate solution to this problem may be found by realizing the calculated supersymmetric relative permittivity via digital grading. The advantage of this method is that it produces a complex relative permittivity function which is constant by parts and can therefore be realized by deposition of the layers of homogeneous materials.

2.2. The formalism of digital grading applied to complex supersymmetric relative permittivity

As explained in the previous section, it is necessary to process the complex supersymmetric relative permittivity by digital grading in order to obtain segments of the structure with homogeneous composition. The digital grading approximation of a complex function is somewhat uncommon; therefore, it will be explained here in detail, assuming that the reader is familiar with the standard digital grading approximation of real functions.

The first step is to define the segment of the structure that will undergo digital grading. Here we select a domain symmetric around zero, as both the real and the imaginary parts of the final function are almost symmetric or anti-symmetric. The area selected for digitalization should not be too wide, in order to ensure the quality of the approximation. The peripheral parts of the function are 'flattened' by taking the average values within particular areas. As shown in equation (21), the value of the initial (constant) relative permittivity may be taken as a satisfactory estimate of that flat outer part of the supersymmetric permittivity. Such averaging of the peripheral area implies that the corresponding field will not be exactly bound, but it will oscillate with sufficiently small amplitude and frequency.

The second step involves the application of digital grading formalism to both the real and the imaginary part of the relative permittivity in the previously defined central area, in the usual manner, as presented in [19–21], with a few modifications.

The conventional digital grading formalism approximates the potentials with only two values (e.g. the maximum and the minimum of the potential) across the whole domain, with the strict layout of those two values. In the procedure applied here, three values are used. This improves the accuracy of the approximation, but complicates the construction of the obtained structure by increasing the number of constituent materials. Supersymmetric relative permittivity is a strongly oscillating function around some average value that is almost equal to the value in bulk or outside of the digitally graded area, so grading with only two values gives poor results and cannot be utilized. Hence, an additional (medium) value is introduced as the average value of the function outside of the digitally graded area, namely as in the 'flattened' area. The higher and the lower value are defined as in [19–21], as the extrema of the function over the entire domain.

As described in [19–21], the complete domain is divided into intervals which are then individually approximated with two different value combinations: the medium and the high value or the medium and the low value. Those intervals will be from now on referred to as the common cells. Thus, the common cell represents a standard interval where the graded approximate function (both the real and the imaginary part) has only two values. The calculated average of $\varepsilon_{ss}(x)$ determines the pair of values which is selected for each common cell. In more detail, the medium and the high value are used to describe a particular cell if the average value of $\varepsilon_{ss}(x)$ within it is greater than the medium value, while the medium and the low value combination is used in the opposite case.

However, the smallest homogenous units intended for depositions are not the segments occupied by individual values in each common cell, but the subcells which will be introduced later.

The width filled with each value within a particular cell depends on the magnitude of the integral

$$S = \int_{\text{Cell}} |\varepsilon_{ss}(x) - \varepsilon_{\text{med}}| \, \mathrm{d}x, \tag{29}$$

where ε_{med} represents one of the two values appearing in a particular cell used as a reference. In this work, by definition, it is always assumed that ε_{med} corresponds to the medium value as it is the only value present in each cell. The width of a non-medium value $w_{\text{high/low}}$, which is either high or low for a specific cell, is defined by the relation

$$w_{\text{high/low}} = \frac{\mathrm{S}}{|\varepsilon_{\text{med}} - \varepsilon_{\text{high/low}}|}. \tag{30}$$

The width occupied by the medium value is thus

$$w_{\text{med}} = d - w_{\text{high/low}}, \tag{31}$$

where d represents the width of the cells.

Finally, in the third step previously obtained real and imaginary digitally graded functions are used to compose the complex digitally graded structure. The complex values are introduced as combinations of real and imaginary values. By combining three real and three imaginary values, nine different complex values are obtained. If the two-value digital grading approximation were used, then such combination would provide 2×2 complex values.

This procedure entails the division of each common cell into subcells so that exactly one complex value can be assigned to each subcell, as shown in figure 2.

The whole structure can thus be constructed in practice by the deposition of the layers of different materials corresponding to each subcell. This implies that each subcell consists of one specific layer of suitable material chosen from the set of nine different materials if three-value digital grading is considered, and from the set of four materials if conventional two-value

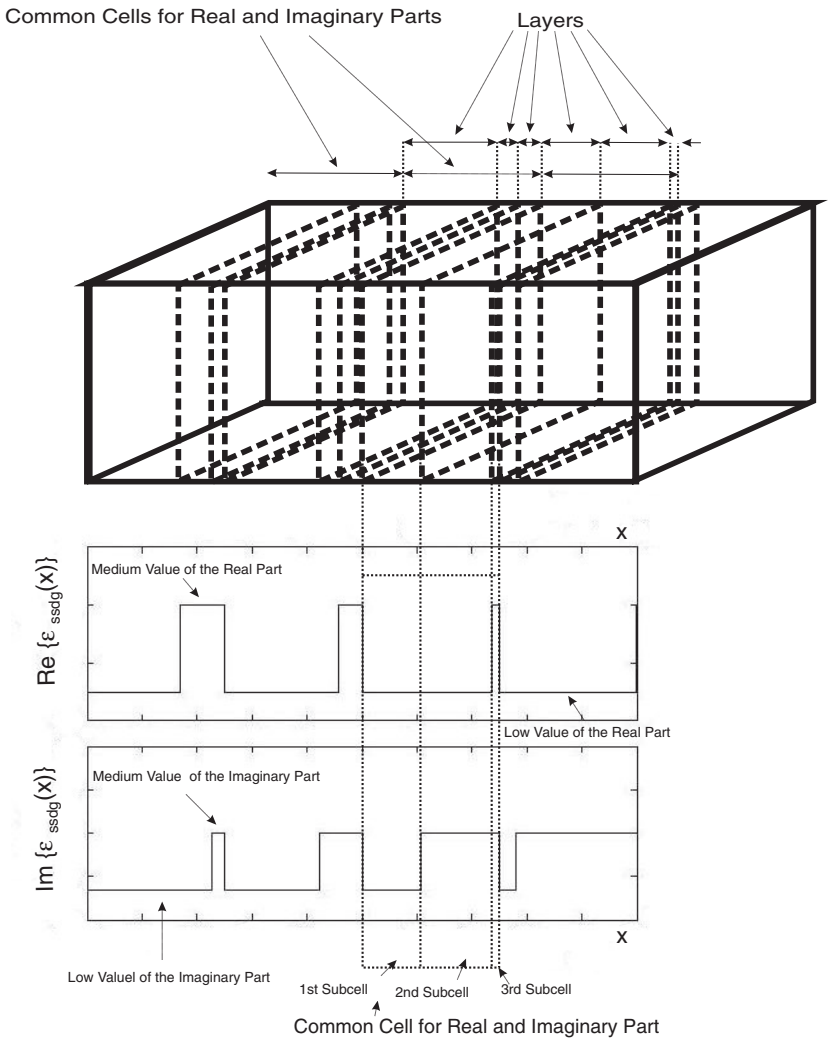

Figure 2. Realization of the complex digitally graded function $\varepsilon_{\mathrm{ssdg}}$. Within one common cell interval of the digitally graded real and imaginary part, three subcells–subintervals are marked by dashed lines. The first subcell is characterized by a combination of the low value real part and low value imaginary part. The second subcell is characterized by a combination of the low value real part and medium value imaginary part. The third subcell is characterized by a combination of the medium value real part and the medium value imaginary part.

digital grading is in use. Because all the cells are shared by the real and the imaginary part of the function (i.e. they characterize both parts at the same time), and each of the cells comprises only two values of the real or the imaginary part, it is evident that the three subcells in each cell are sufficient to obtain the satisfactory complex digitally graded function.

3. Numerical examples and discussion

Depending on the selection of values of ν, ε, λ_0 and μ for the flat optical potential, various supersymmetric optical potentials are obtained. One can take for example $k = 3\ \mathrm{mm}^{-1}$, $\varepsilon = 5$, $\mu = 1$, $\lambda_0 \approx 630\ \mu\mathrm{m}$, where $k_0 = \omega_0/c = 2\pi/\lambda_0$ denotes the wavenumber

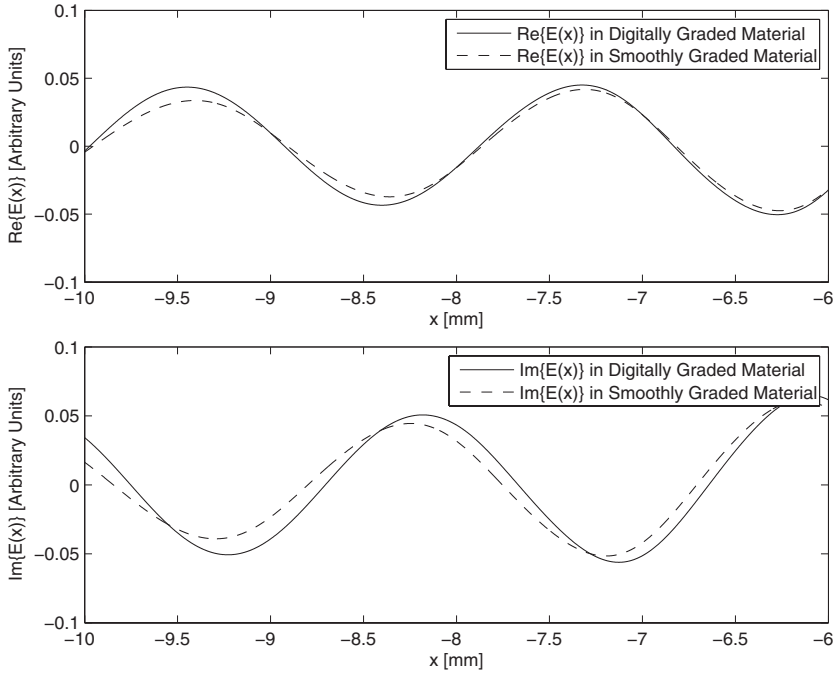

Figure 3. Comparison of the electric fields in the initial (smoothly graded) optical potential and the digitally graded optical potential. The initial conditions are the same within the central parts of the structures, so the differences between the approximated and the 'accurate' electric field functions are very small therein. The biggest difference appears at the end of the domain, which is here enlarged for clarity.

outside of the digitally graded area (in the homogenous part, which can be considered in the limit $x \to \pm\infty$), with the relative permittivity $\varepsilon_{ss} = \varepsilon$ and the permeability $\mu_{ss} = \mu$ as $\Theta ss(x \to \pm\infty) = -k_0^2\varepsilon\mu$. The wavenumber k defines the eigenvalue ν for which the SUSY formalism is employed. The remaining parameters are then calculated as $k_0 = 10\ \text{mm}^{-1}$, $\nu = -\beta^2 = k^2 - k_0^2\varepsilon\mu = -491\ \text{mm}^{-2}$. In addition, C and ρ are defined so that the supersymmetric eigenfunction is normalizable:

$$C = 3 + 3\text{i}, \qquad \rho = 9\ \text{mm}. \tag{32}$$

In the numerical example treated here, three real and three imaginary values of relative permittivity are calculated:

$$\begin{aligned} &\text{Re}(\varepsilon_{\text{high}}) = 5.1513, \qquad \text{Re}(\varepsilon_{\text{med}}) = 5, \qquad \text{Re}(\varepsilon_{\text{low}}) = 4.9318, \\ &\text{Im}(\varepsilon_{\text{high}}) = 0.158\,71, \qquad \text{Im}(\varepsilon_{\text{med}}) = 0, \qquad \text{Im}(\varepsilon_{\text{low}}) = -0.155\,65. \end{aligned} \tag{33}$$

The combinations of these values yield nine different homogenous materials whose relative permittivity values are

$$\begin{aligned} &\varepsilon_{\text{ssdg1}} = 5.1513 + \text{i} \cdot 0.158\,71, \qquad \varepsilon_{\text{ssdg2}} = 5.1513, \qquad \varepsilon_{\text{ssdg3}} = 5.1513 - \text{i} \cdot 0.155\,65, \\ &\varepsilon_{\text{ssdg4}} = 5 + \text{i} \cdot 0.158\,71, \qquad \varepsilon_{\text{ssdg5}} = 5, \qquad \varepsilon_{\text{ssdg6}} = 5 - \text{i} \cdot 0.155\,65, \\ &\varepsilon_{\text{ssdg7}} = 4.9318 + \text{i} \cdot 0.158\,71, \qquad \varepsilon_{\text{ssdg8}} = 4.9318, \qquad \varepsilon_{\text{ssdg9}} = 4.9318 - \text{i} \cdot 0.155\,65. \end{aligned} \tag{34}$$

This combination of parameters is not exclusive. The set of parameters given by equation (34) is just an illustration, and this example is generated so that the values of the real and imaginary

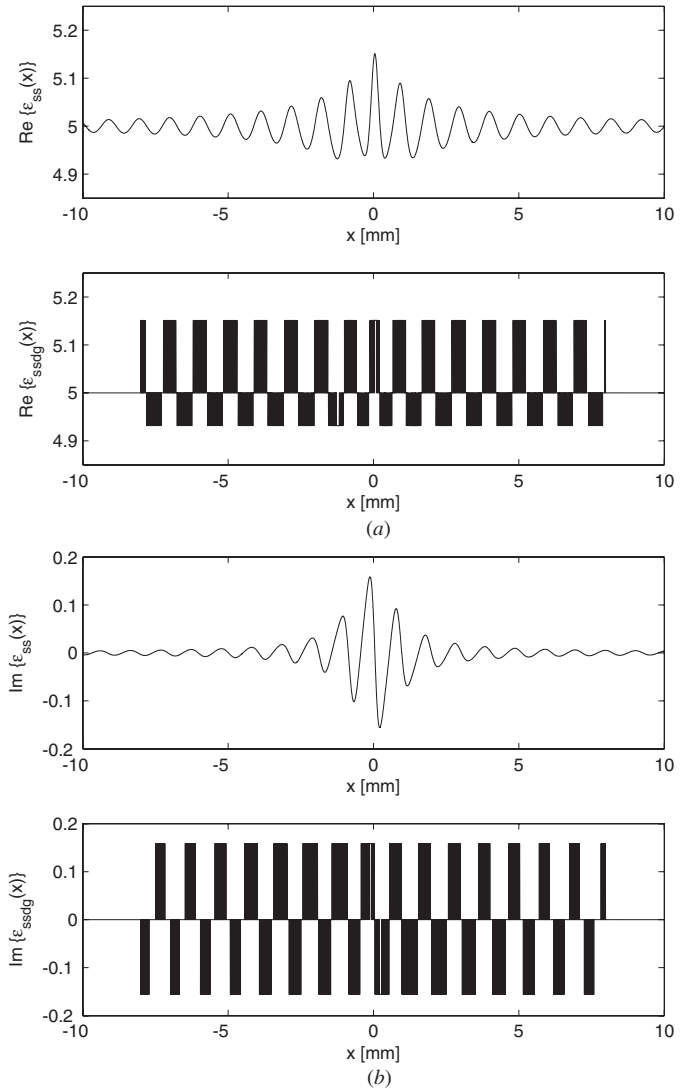

Figure 4. The results of the digital grading approximation with three values for both (*a*) the real and (*b*) the imaginary part.

parts of dielectric permittivities are within realizable limits, the condition that can obviously be satisfied by other parameter combinations. As already pointed out, some materials must have the negative imaginary part of the dielectric permittivity, which categorizes them as active dielectrics—materials which are nowadays extensively studied and their realization and characterization are well documented [22–24]. In our opinion, there is an additional approach to the realization of materials described by equation (34). It relies on (electrically or optically driven) quantum systems such as the quantum cascade laser, quantum amplifier or multiple quantum wells (dots), which exhibit different values of dielectric permittivity from the background permittivity [23, 24]. The sign and magnitude of the real and imaginary parts of this resultant permittivity depend on the design of the quantum structure in question (e.g.

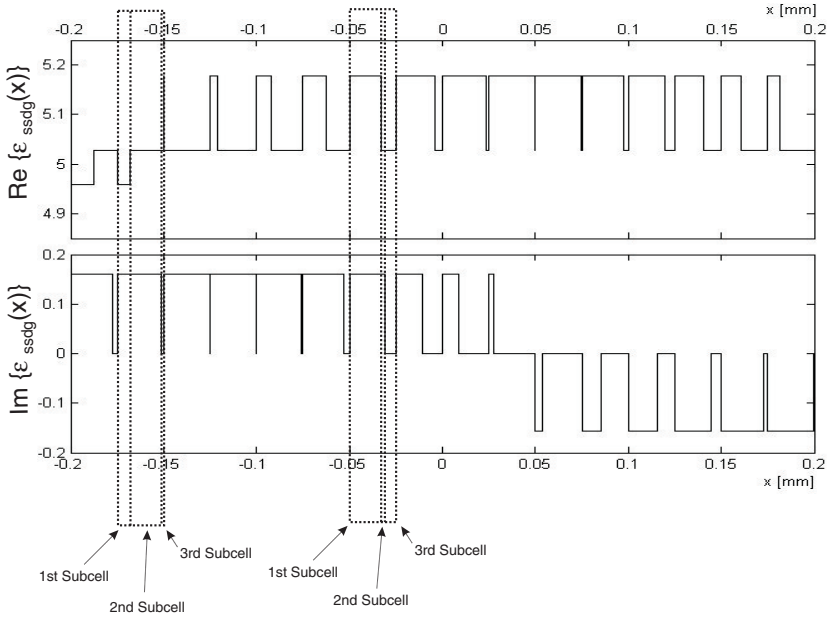

Figure 5. Magnified section of the digitally graded supersymmetric relative permittivity (the real and imaginary part). Two arbitrarily chosen common cells with their subcells are marked by the dotted lines: the first subcell of the left selected cell is described by the material with the high imaginary and low real value, namely $\varepsilon_{\text{ssdg7}} = 4.9318 + \text{i} \cdot 0.158\,71$; the second subcell of the left selected cell is represented by the material with the high imaginary and medium real value, i.e. $\varepsilon_{\text{ssdg4}} = 5 + \text{i} \cdot 0.158\,71$; the third subcell of the left selected cell corresponds to the material with $\varepsilon_{\text{ssdg5}} = 5$. The first subcell of the right selected cell corresponds to the material with the high imaginary and high real value, that is $\varepsilon_{\text{ssdg1}} = 5.1513 + \text{i} \cdot 0.158\,71$; the second subcell of the right selected cell is described by$\varepsilon_{\text{ssdg4}} = 5 + \text{i} \cdot 0.158\,71$; and finally, the third subcell of the right selected cell is described by $\varepsilon_{\text{ssdg5}} = 5$.

on widths of the well and the barrier layers, and on the material composition). For instance, materials with indices 3, 6 and 9 from equation (34) may be created so as to have predefined dielectric constants at a given frequency by varying e.g. only the layer widths, within relatively narrow limits, since these permittivities are quite similar. Apparently, the same applies for the group of materials with indices 1, 4, and 7, as well as 2, 5 and 8.

Depending on the wavelength of the electromagnetic mode, the dimension of the whole structure in the x-direction can be varied. The minimal thickness of an individual layer within the generated structure is limited by the numerical step used in calculations, which is here set to $d = 1\ \mu$m. The obtained results are presented in figures 3–5.

4. Conclusion

The SUSY method was used to generate the complex optical potential with a localized electric field state in the continuum part of the spectrum. The bound state eigenvalue can be chosen arbitrarily from the continuous spectrum of an initial operator $\widehat{N}_1$. The non-Hermitian operator $\widehat{N}_3$, with a complex potential, is then generated as almost isospectral to $\widehat{N}_1$, with an exception of one additional localized state with normalizable eigenfunction. The parameters of the complex optical potential have to be chosen so as to satisfy the condition of normalizability

for this electric field function. The obtained smooth structural profile is then processed by the digital grading technique, adapted to the case of a strongly oscillating complex function of the real argument. Thus, the values of the complex relative permittivity are approximated so that the structure may be realized by compiling the layers of homogeneous materials.

Acknowledgments

This work was supported by the Ministry of Science (Republic of Serbia), ev. no. 141006. VM and JR also acknowledge the financial support from NATO Collaborative Linkage Grant (reference CBP. EAP.CLG 983316).

Appendix

The new Wronskian function is defined as

$$W(x) = \overline{u_v}(x)\frac{\mathrm{d}u_n(x)}{\mathrm{d}x} - u_n(x)\frac{\mathrm{d}\overline{u_v}(x)}{\mathrm{d}x} \tag{A.1}$$

where $\overline{u_v}(x)$ consists of two linearly independent parts:

$$\overline{u_v}(x) = u_v(x)\left[1 + C\int_{(x)}\frac{\mathrm{d}x}{u_v^2(x)}\right] = u_v(x) + Cu_v(x)\int_{(x)}\frac{\mathrm{d}x}{u_v^2(x)} = u_v(x) + C\tilde{u}_v(x). \tag{A.2}$$

Thus we obtain

$$W(x) = u_v(x)\frac{\mathrm{d}u_n(x)}{\mathrm{d}x} - u_n(x)\frac{\mathrm{d}u_v(x)}{\mathrm{d}x} + C\left[\tilde{u}_v(x)\frac{\mathrm{d}u_n(x)}{\mathrm{d}x} - u_n(x)\frac{\mathrm{d}\tilde{u}_v(x)}{\mathrm{d}x}\right]. \tag{A.3}$$

Further, the function $u_n(x)$ also comprises two linearly independent parts:

$$u_n(x) = u_{n1}(x) + u_{n2}(x) \tag{A.4}$$

where $\lim_{\nu_n\to\nu} u_{n1}(x) = u_\nu(x)$ and $\lim_{\nu_n\to\nu} u_{n2}(x) = \tilde{u}_\nu(x)$. Therefore, in the case of $\nu_n \to \nu$ and $u_n(x) = u_{n1}(x)$, equation (A.3) amounts to

$$W(x) = C\left[\tilde{u}_\nu(x)\frac{\mathrm{d}u_\nu(x)}{\mathrm{d}x} - u_\nu(x)\frac{\mathrm{d}\tilde{u}_\nu(x)}{\mathrm{d}x}\right] = \text{const} \quad \text{q.e.d.} \tag{A.5}$$

while in the other case $u_n(x) = u_{n2}(x)$, it reads

$$W(x) = u_\nu(x)\frac{\mathrm{d}\tilde{u}_\nu(x)}{\mathrm{d}x} - \tilde{u}_\nu(x)\frac{\mathrm{d}u(x)}{\mathrm{d}x} = \text{const} \quad \text{q.e.d.} \tag{A.6}$$

The conclusion is that all the eigenfunctions for $\nu_n \neq \nu$ which are double-degenerate become merged into one eigenfunction $\overline{u_\nu}(x)$ in the limit $\nu_n \to \nu$.

References

[1] von Neumann J and Wigner E 1929 *Phys. Z.* **30** 465–70
[2] Stillinger F H and Herrick D R 1975 *Phys. Rev.* A **11** 446–54
[3] Stillinger F H 1976 *Physica* **B&C 85** 270–6
[4] Herrick D R 1976 *Physica* B **85** 44–50
[5] Robnik M 1979 *J. Phys. A: Math. Gen.* **12** 1175–80
Robnik M 1986 *J. Phys. A: Math. Gen.* **19** 3845–8
[6] Weber T A 1999 *J. Math. Phys.* **40** 140–9
[7] Pursey D L and Weber T A 1995 *Phys. Rev.* A **52** 4255–8
[8] Capasso F, Sirtori C, Faist J, Sivco D L, Chu S-N G and Cho A Y 1992 *Nature* **358** 565–7
[9] Pappademos J, Sukhatme U and Pagnamenta A 1993 *Phys. Rev.* A **48** 3525–31
[10] Sree Ranjani S, Panigrahi P K and Kapoor A K 2008 arXiv: cond-mat/0806.1799

[11] Sree Ranjani S, Kapoor A K and Panigrahi P K 2008 *J. Phys. A: Math. Theor.* **41** 285302
[12] Petrovic J S, Milanovic V and Ikonic Z 2002 *Phys. Lett.* A **300** 595–602
[13] Milanovic V and Ikonic Z 2002 *Phys. Lett.* A **293** 29–35
[14] Bulgakov E N and Sadreev A F 2008 *Phys. Rev.* B **78** 075105
[15] Marinica D C, Borisov A G and Shabanov S V 2008 *Phys. Rev. Lett.* **100** 183902
[16] Joannopoulos J D, Meade R D and Winn J N 1995 *Photonic Crystals: Molding the Flow of Light* (Princeton, NJ: Princeton University Press)
[17] Bhat N A R and Sipe J E 2006 *Phys. Rev.* A **73** 063808
[18] Bhat N A R and Sipe J E 2001 *Phys. Rev.* E **64** 056604
[19] Vlaev S, Garcia-Moliner F and Velasco V R 1995 *Phys. Rev.* B **52** 13784–7
[20] Lee J H, Li S S, Tidrow M Z, Liu W K and Bacher K 1999 *Appl. Phys. Lett.* **75** 3207–9
[21] Mathine D L, Maracas G N, Gerber D S, Dropad R, Graham R J and McCartney M R 1994 *J. Appl. Phys.* **75** 4551–6
[22] Shalaev V M 2007 *Nat. Photonics* **1** 41–8
[23] Ginzburg P and Orenstein M 2008 *J. Appl. Phys.* **103** 083105
[24] Ginzburg P and Orenstein M 2008 *J. Appl. Phys.* **104** 063513